THE APPLICATION OF NESTED DISSECTION TO THE SOLUTION OF A 2.5D ELECTROMAGNETIC PROBLEM

G. H. SMITH[1], P.R.WILLIAMSON[2] AND K. VOZOFF[3]

Abstract

We use the method of nested dissection to solve a 2.5D finite difference electromagnetic problem. This method is considered in some detail, and we have found that the expected theoretical run time savings over more common methods are realised in practice. The program has been used to model EM propagation in coal seams with a view to detecting seam disruptions, which can cause a loss of production in longwall mining operations. Various experimental results and a field survey are discussed and we are able to use these results to construct a physically reasonable model which explains the field data. Some further realistic geological structures are modelled and a comparison between our modelling program and several independent methods shows satisfactory agreement.

1 Introduction

1.1 Kron (1955) proposed and demonstrated an approach to solving the equations for a network which was too big to fit in its entirety onto the calculating machines then available: he divided ('tore', hence the name 'diakoptics') it up into subnetworks which could be accommodated, solved them and finally reconnected these sub-solutions to form a 'junction network'. This was not sparse, but had many fewer nodes than the original network and could be solved directly, using standard algorithms. This procedure was further expounded and formalised by Savage and Kesavan (1980). An approach to elimination ordering which appears to use similar ideas in a recursive fashion on the matrix graph, entitled 'nested dissection' was presented in George (1973). This and subsequent work (e.g. George, 1977) showed that this ordering is potentially considerably more efficient for those matrices with the topology of 2- or 3- dimensional finite difference or finite element boundary value problems than the standard row-by-row ordering which generates the familiar banded matrices. However this technique appears to have been largely overlooked, presumably because of its relative complexity in programming or uncertainty as to its stability in practice.

In this paper we demonstrate the application of these concepts from graph theory to the solution of a practical problem in electromagnetic geophysics.

1.2 Modelling problems of geophysics generally deal with the response of a halfspace or wholespace to some source field. The space may be uniform or made up of regions - horizontal layers or more complicated geometries - having different physical properties representing different rock types or conditions. The source may be a plane wave incident from above, or a multipole on, in or above the halfspace or within a wholespace. Historically the problems arise in petroleum, mineral, geothermal and groundwater exploration, or in design of dams, bridges and other structures. Increasingly they arise in planning production from coal and metal mines, oil wells and in a variety of environmental applications.

1 Department of Mathematics, University of Technology, Sydney

2 Department of Geology, Imperial College, London, formerly at the centre for Geophysical Exploration Research, Macquarie University, Sydney

3 Centre for Geophysical Exploration Research, Macquarie University, Sydney

To describe the degree of complexity of a particular structure it is useful to introduce fractional dimensions. If the physical properties of a model vary in two dimensions and the source is a point source, then the phase and amplitude of the fields will vary in three dimensions. In a sense, this model lies between a 2D model with a line source, in which both fields and physical properties vary in two dimensions only, and a full 3D model. We classify this as a 2.5D model. 2D, 2.5D and 3D problems usually have to be attacked numerically, although a few important analytic solutions are known.

One currently important problem is that of wave propagation in coal seams which are disturbed geologically. As will be indicated, in many environments coals seams are relatively unusual in their properties compared to the rocks above and below. They have much lower seismic velocities and have much higher resistivities. Thus if they are undistorted by subsequent geological processes they form natural waveguides. These are ideal for large scale automated mining (called 'longwall' mining) operations. A typical longwall operation in Australia produces $1M worth of coal in 3-4 days uninterrupted operation. However when the machinery encounters a geological irregularity such as a fault or intrusive in the seam, coal production is lost, for a month or more, and the machinery, costing upwards of $20M, can be damaged.

Disturbances in the seams disrupt their waveguide characteristics. They locally reduce elastic wave velocities and, by allowing water to penetrate, reduce electrical resistivities. To detect such irregularities in advance, elastic wave measurements have been used for 10-15 years with considerable success, since the irregularities introduce scatterers into the otherwise simple elastic waveguide. However such 'in-seam seismic' surveys tend to be slow and expensive, since holes must be drilled to allow both sources and receivers to make direct physical contact with the coal.

More recently the use of medium frequency EM fields was introduced, for example in the paper by Emslie and Lagace (1976) and the radio imaging method (RIM) of Stolarczyk (1986). These involve horizontal magnetic dipoles consisting of small portable loops, or vertical electric dipoles, which are equally portable. Neither requires physical contact with the rocks.

In both types of surveys it is often easier to make the measurements than to interpret them. 2D modelling for the elastic wave problem was implemented several years ago (Drake et al, 1984, Edwards et al, 1985), and is now used routinely. Modelling for the EM problem was begun more recently. Publications include analytical solutions for unperturbed coal seams by Hill (1984, 1986), numerical solutions for unperturbed seams (Shope et al, 1986; Shope, 1987; and Stolarczyk, 1986) and numerical solutions for perturbed seams (Greenfield and Wu, 1988). A general description of our numerical modelling results has been submitted for publication (Liu, et al. 1991).

To account for the complexity of geological structures it is sometimes desirable to carry out full 3D modelling (Hohmann, 1988), but this is computationally expensive and often unnecessary. In this paper we deal with the 2.5D finite difference problem, in which the source is a horizontal magnetic dipole in the x-direction and the physical properties change in y and z but are invariant in x. (The direction in which properties are invariant is known as the **strike direction**.) This was the geometry used by Stoyer and Greenfield (1976). In particular we describe the use of Nested Dissection (George, 1973) for more efficient inversion of the sparse matrices arising in the finite difference formulation.

2 Physical properties and experimental results

There are few published values for the electromagnetic properties of coals, in part because there are such a wide variety. These range from very low grade, peaty lignites (brown coal) hardly distinguishable from garden loam, to high grade anthracite, which can be electrically conductive. The coals of interest to us are medium grade bituminous, found throughout Eastern Australia but also commonly in many other parts of the world. Laboratory measurements on wet specimens (as

in nature) made at frequencies in the 0.1 - 1.0 MHz range give conductivities of 0.0001 to 0.001 S/m. Typical conductivities for the sedimentary beds above and below the coals range from 0.001 to 0.3 S/m, so that in some exceptional situations the conductivity contrast does not support wave guiding.

Coal seam thicknesses range from nil to more than 10 m, with 1 - 3 m being the most common for coal mining.

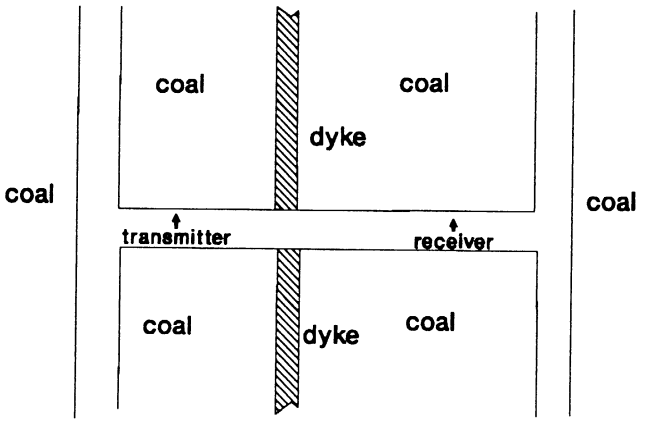

Figure 2.1 Plan view of a survey configuration for Kemira Colliery, NSW (Hatherly, 1987). The transmitter and receiver are vertical coplanar loops and the measurements are taken along a single mine roadway. The effect of the roadway may be neglected.

A typical survey configuration is shown in figure 2.1, while the results from this survey are shown in figure 2.2 (Hatherly, 1987). Also included in figure 2.2 are computed amplitudes at 300 kHz, for comparison with the survey data. The coal seam here is known to be 6 m thick. To fit the observed attenuation rate, conductivities of rock and coal are 0.003 and 0.0003 S/m respectively. The discontinuity in the model and the observed data near 75 m is due to an intrusive conductive dyke, a 2 metre thick, near-vertical body of rock injected at high temperature. Where this comes in contact with the coal, the latter is converted to highly conductive cinder, which reflects electromagnetic energy and disrupts the waveguide. The intrusive rock itself is usually very hard and may or may not be conductive, according to its water content. Intrusive dykes are a common occurrence in many coal fields, so it is important that they can be detected well in advance of mining. It is the effects of such features on electromagnetic signal propagation that we wish to predict.

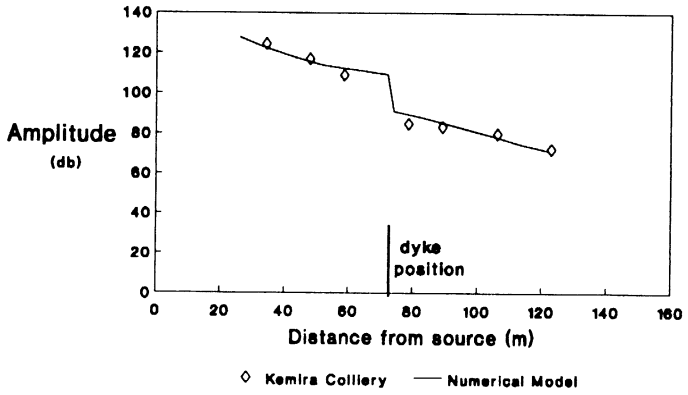

Figure 2.2 Comparison between computed values and field measurements for Kemira Colliery, NSW, (Hatherly, 1987). The transmitter is fixed 72m to the left of the dyke as the receiver moves away to the right.

3 Methods

The solution of the modelling problem outlined in the introduction requires the use of Maxwell's equations for the electromagnetic field quantities **E** and **H**. For an $e^{i\omega t}$ time dependence these equations are

$$\nabla \times \mathbf{E} = -i\omega\mu(\mathbf{H} + \mathbf{M}_s) \tag{3.1}$$

$$\nabla \times \mathbf{H} = \sigma'\mathbf{E} + \mathbf{J}_s \quad , \tag{3.2}$$

where $\mathbf{M}_s$ and $\mathbf{J}_s$ are magnetic and electrical source terms respectively and $\sigma' = \sigma + i\omega\varepsilon$.

In most of the classes of model encountered equations (3.1) and (3.2) cannot be solved using analytic methods. Instead, the solution requires the finite difference, finite element or integral equation approaches (Hohmann, 1988). As is well known, the finite difference and finite element methods are computationally intensive, and the numerical burden increases rapidly with the size of the model (i.e. the number of nodes). The system of linear equations which results from such modelling in the frequency domain can be cast into the form of a standard sparse matrix inversion. This may be accomplished either by direct factorization (Gaussian elimination) or by some kind of iterative method. Although the latter can be relatively efficient for one-off solutions, the factorization comes into its own in the context of some kinds of inversion. In particular, when the calculation of the Fréchet partial derivatives may be achieved by repeated solution of the same matrix equation for a variety of right hand sides the factorization option is very efficient and elegant (Jupp and Vozoff, 1977). It is similarly attractive for modelling the responses to several source configurations. However, even while taking advantage of this efficiency in inversion of a small (11×9) 2-D grid,

Jupp and Vozoff (1977) report that the factorization and subsequent solutions dominate the requirements of their magnetotelluric inversion program, accounting for 75% of the total CPU time. Furthermore this percentage will increase with the number of points in the model mesh, whether it remains two-dimensional or expands into the third, so an increase in the efficiency of inversion would have an almost equal effect on the whole inversion.

One tool which has been used to study the factorization of sparse matrices is graph theory (e.g. Bunch and Rose, 1974). This gives a picture of the topology of the matrix at any stage of an elimination (factorization) procedure and thereby allows one to keep track of the destruction of zeros, or 'fill-in', in the factor, which is a strong indicator of the efficiency of the procedure. The initial graph of a finite difference matrix corresponds to the network analogue constructed for engineering or field problems (e.g. Madden, 1972), and the evolution of the graph follows the equivalent networks as nodes are removed.

In order to find solutions to equations (3.1) and (3.2) we select a right handed set of Cartesian axes with the x-axis pointing in the strike direction and the z-axis vertically downwards. Following Stoyer and Greenfield (1976) we take Fourier transforms of these equations along the x-axis. For $\mathbf{E}$ the Fourier transform pair is

$$\hat{\mathbf{E}}(k_x, y, z) = \int_{-\infty}^{\infty} \mathbf{E}(x, y, z) e^{-ik_x x} dx \tag{3.3}$$

$$\mathbf{E}(x, y, z) = \frac{1}{2\pi} \int_{-\infty}^{\infty} \hat{\mathbf{E}}(k_x, y, z) e^{+ik_x x} dk_x \tag{3.4}$$

with corresponding expressions for $\mathbf{H}$. Assume that the source is a horizontal magnetic dipole in the x-direction and substitute these results into equations (3.1) and (3.2). Then we find after some calculation that the problem can be formulated in terms of the following two coupled second order partial differential equations for $\hat{E}_x$ and $\hat{H}_x$, the components of $\hat{\mathbf{E}}$ and $\hat{\mathbf{H}}$ in the strike direction:

$$-\frac{\partial}{\partial y}\left(\frac{1}{Z^M}\frac{\partial \hat{H}_x}{\partial y}\right) - \frac{\partial}{\partial z}\left(\frac{1}{Z^M}\frac{\partial \hat{H}_x}{\partial z}\right) - ik_x\left(\frac{\partial \hat{E}_x}{\partial z}\frac{\partial \xi}{\partial y} - \frac{\partial \hat{E}_x}{\partial y}\frac{\partial \xi}{\partial z}\right) + \mathcal{Y}^M \hat{H}_x = -\mathcal{Y}^M \hat{M}_x \tag{3.5}$$

$$-\frac{\partial}{\partial y}\left(\frac{1}{Z^E}\frac{\partial \hat{E}_x}{\partial y}\right) - \frac{\partial}{\partial z}\left(\frac{1}{Z^E}\frac{\partial \hat{E}_x}{\partial z}\right) + ik_x\left(\frac{\partial \hat{H}_x}{\partial z}\frac{\partial \xi}{\partial y} - \frac{\partial \hat{H}_x}{\partial y}\frac{\partial \xi}{\partial z}\right) + \mathcal{Y}^E \hat{E}_x = -\hat{J}_x \tag{3.6}$$

where $k^2 = -i\omega\mu\sigma'$, $Z^M = \sigma'(1 - k_x^2/k^2)$, $Z^E = i\omega\mu(1 - k_x^2/k^2)$, $\mathcal{Y}^M = i\omega\mu$, $\mathcal{Y}^E = \sigma'$ and $\xi = (k_x^2 - k^2)^{-1}$. In this way we reduce the problem to a 2D one for each value of k_x. Furthermore, the unknown components $\hat{E}_x$ and $\hat{H}_x$ are continuous making it unnecessary to set up gradational boundaries at conductivity discontinuities within the grid.

3.1 Finite Difference Scheme

Equations (3.5) are solved by using a 5-point difference scheme. The cross-section of the 2-D geological model is represented by a rectangular grid, where the spacing of the nodes need not be uniform. Values of $\hat{H}_x$ and $\hat{E}_x$ are computed at each node. We use an area discretization for the parameters σ, ε and μ by specifying their values for each rectangular element bounded by the grid lines. These values are kept constant within the element. At a typical node (i,j) we integrate equations

(3.5) and (3.6) over the area shown in figure 3.0. The integrals can be expressed as contour integrals around the boundary in which only the normal derivatives of the fields arise and for which central difference approximations can be used.

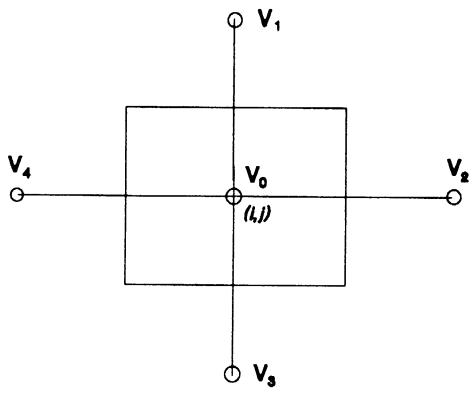

Figure 3.0 The figure shows 4 nodes surrounding a typical node (i,j). V denotes either $\hat{H}_x$ or $\hat{E}_x$. Equations (3.5) and (3.6) are integrated over the rectangular area shown.

For an $m \times n$ grid there are mn difference equations corresponding to equation (3.5) and mn difference equations corresponding to equation (3.6). At a generic node, the difference equations are of the form

$$\sum_{i=1}^{4}\left\{\frac{\hat{H}_{x0}-\hat{H}_{xi}}{Z_i^M}+\frac{\hat{E}_{xi}-\hat{E}_{x0}}{C_i}\right\}+\mathcal{Y}_0^M\hat{H}_{x0}=S_0^M \tag{3.7}$$

$$\sum_{i=1}^{4}\left\{\frac{\hat{E}_{x0}-\hat{E}_{xi}}{Z_i^E}-\frac{\hat{H}_{xi}-\hat{H}_{x0}}{C_i}\right\}+\mathcal{Y}_0^E\hat{E}_{x0}=S_0^E \quad , \tag{3.8}$$

where the C_i represent coupling terms.

The resulting $2mn$ equations can be written in a form having a block tridiagonal coefficient matrix (see appendix), but will in fact be ordered for solution using the previously mentioned nested dissection method which we describe in more detail below.

It is necessary to keep grid spacing near the source to about one sixth of a skin depth. For general purposes, grid spacings of 1 metre are maintained near the source and kept to 6 metres or less within the area of interest. Towards the sides and top of the grid, spacings are rapidly increased away from the area of interest. A plane wave terminal impedance boundary condition was found to be adequate for all grid edges. In the coal seam waveguide mode the fields fall away rapidly as we move vertically away from the coal seam so that typically we use a short, wide grid (30×80).

Having solved equations (3.5) and (3.6) for $\hat{E}_x$ and $\hat{H}_x$ using a number of k_x values, we use equation (3.4) to return to the space domain. In practice we found that for a 2 - 6 metre coal seam a choice of $k_x = 0$ together with 15 other values logarithmically spaced at 4 samples per decade was adequate for frequencies in the range 200 - 700 kilohertz. By using appropriate symmetry or skew symmetry, field values for negative k_x can be obtained. Intermediate values for the Fourier transforms of the fields are approximated by a cubic spline which can be integrated to give the inverse transform.

3.2 Tearing Methods and Nested Dissection

The numerical solution of equations (3.5) and (3.6) will dominate the entire modelling program in terms of CPU time and storage requirements for models of a useful size. This can be seen by considering an $n \times n$ 2D gridpoint model: the effort to set up the equations and interpret the results will typically increase linearly with the number of gridpoints i.e. as n^2. A standard form of these equations results from a row-by-row ordering of the nodes with the electric and magnetic equations for each node taken consecutively; the matrix representation is then block tridiagonal with each $2n \times 2n$ off-diagonal block being 2×2 block diagonal and each $2n \times 2n$ diagonal block being block tridiagonal. This would require about $8n^4$ multiplications to factorize by elimination and $4n^3$ storage locations for the factor i.e. between $4n^3$ and $8n^3$ multiplications for each solution after factorisation depending on the source location. Thus as n increases the proportion of the effort devoted to the factorization and solutions of these equations will sooner or later be overwhelming. The absolute requirements will also be very large, and will eventually exceed the capabilities of any machine. This problem is even more acute in 3D, where for an n^3 model factorization is $O(n^7)$ and storage $O(n^5)$ for a the corresponding matrix. Clearly any reduction in the multiplication count and storage requirements here may have a significant impact on the expected cost of running the program for a given size, and conversely extend the range of effects which can be modelled within the constraints of the available resources.

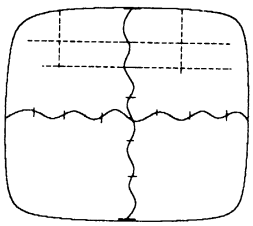

Figure 3.1 Schematic representation of the tearing of a network into four subnetworks. The wavy lines indicate the positions of the tears and points of tearing define the nodes of the resultant junction network.

In 1955 Kron proposed a method for solving networks which were too large for solution by direct application of conventional methods on the calculating machines then in use. This involved 'tearing up' the network into subnetworks which **could** be directly solved, and then coupling these solutions together to form a 'junction network' which is also small enough to be solved. To illustrate this, consider the example of the schematic network shown in figure 3.1. By tearing along the wavy lines shown, four subsystems are created, along with the topology of the junction network . These subsystems are inverted separately, and their solutions reconnected at the points of tearing to form the full junction network. This is a microcosm of the whole network in that it behaves exactly as the original did at those points, but is of considerably reduced dimension. The key to this process is the validity of the theory of Multi-Terminal Representations (MTRs) which was articulated by Savage and Kesavan (1980) in their recapitulation and reformulation of Kron's work. Although they differ slightly in language and emphasis, the theory of MTRs is essentially equivalent to that of Diakoptics, cf. Kesavan and Dueckman, (1982). The central postulate of this theory is that 'an n-terminal component (subsystem) can be characterized by (n-1) independent equations in (n-1) pairs of complementary variables where these variables are specified by an oriented tree graph that connects all the interconnection nodes'. That is, the response of any subsystem to stimuli at the tearing points, as seen at these points, and so its effect on the remainder of the network, can be fully described by a network involving only these nodes, no matter how complicated the 'inner' part of the subsystem

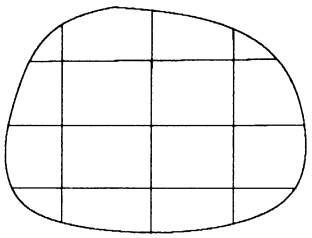

Figure 3.2 The graph of a subnetwork produced by tearing; in this case the boundary is assumed to be completely defined by tearing so that the points where the network contacts this boundary will become nodes of the multiterminal graph of the subnetwork.

For example the graph of a subsystem shown in figure 3.2 may be represented by the multi-terminal graph of figure 3.3 after appropriate calculations have been performed to derive the network equations for the new graph. Such MTG's may then be connected, as shown in figure 3.4, to yield a new representation of the entire network. The resultant system of equations is typically much smaller (but less sparse) than the original ($2n$ square rather than n^2), so that factorization is relatively cheap ($O(n^3)$ rather than $O(n^4)$). This is only true for networks of relatively low connectivity, so that the degree of each node is much less than the number of nodes; fortunately this condition is satisfied in most physical applications, where direct interactions are purely local. The overall numerical benefit of the tearing/reconnection procedure in our schematic example, if done carefully, should be a reduction of about half in the leading order term of the multiplication count, albeit at the cost of larger lower-order terms. Further reduction is in principle obtainable by finer tearing, but the main computational benefits espoused by Kron (1955, 1963) may be summed up as the flexibility conferred by the procedure. In particular one might solve several such networks with common subnetworks connected in different configurations at little extra cost; repeated subnetworks only need to be solved once, and to solve a network which is only different in one region from one

previously solved may involve only the re-solution of the relevant subnetwork and the junction network connecting it to the rest of the network. This latter fact may be of use in modelling when examining the effect of changing the properties of a particular zone (cf. Brewitt-Taylor and Johns, 1978), or in corresponding styles of inversion. However Brewitt-Taylor and Johns encountered a significant overhead in their initial modelling run; this was partly due to the fact that they did not tear for numerical efficiency, and presumably also because of the organisational work involved in setting up the matrices for solution, which Kron effectively performed by hand. Finally, an entire network, having been solved diakoptically, may be taken as a subnetwork in a larger network, and so on to the point where the full network would exceed the limits of the computer; this may be relevant in 3-D modelling.

Kron and other advocates of diakoptic methods emphasize the distinction between tearing and matrix partitioning. One aspect of this is the fact that the incidence/connection matrices, which correspond in a sense to off-diagonal blocks, are purely topological. However the graphical representation of matrices (see e.g. Bunch and Rose, 1974) enables one to point out the strong similarities: a symmetric (Hermitian) matrix is represented by a graph with a node for each row/column and edges connecting nodes corresponding to each pair of off-diagonal non-zero entries i.e. the graph contains an edge between nodes i and j if the ijth (and so the jith) element of the matrix is non-zero. Therefore a typical finite difference matrix for a rectangular region has a rectangular grid graph (see figure 3.5).

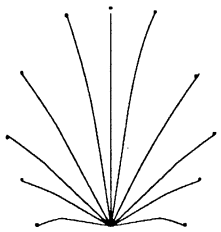

Figure 3.3 The multiterminal graph of the subnetwork in figure 3.2.

Partitioning the matrix then appears to effect something similar to tearing on the graph. The process of Cholesky factorization of the matrix by Gaussian elimination is represented by sequentially deleting each node and its incident edges and adding edges between remaining pairs of nodes which were previously unconnected but mutually connected to the eliminated node (see figure 3.6). Then the number of multiplications (or divisions) performed for the factorization is given by

$$M_{fact} = \sum_{nodes} d_i(d_i + 1)$$

where d_i is the degree of (number of edges incident on) the node at the time of its elimination; the number of non-zero entries in the factor, which is equal to half the number of operations to solve for a given right hand side after factorization, is

$$\frac{1}{2}M_{sol} = \sum_{nodes} (d_i + 1) \quad .$$

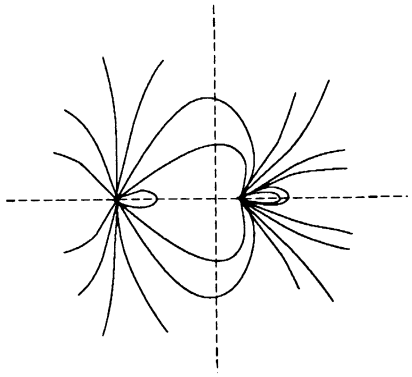

Figure 3.4 Part of a graph of a typical junction network, composed of the union of the MTG's of several subnetworks.

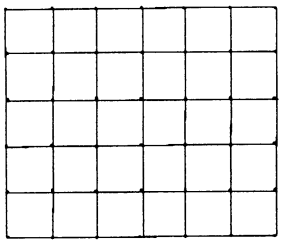

Figure 3.5 Graphical representation of a typical finite difference matrix.

The d_is, and therefore the operation counts above, may be significantly affected by the elimination order i.e. the permutation of the matrix (note that all permutations have the same initial graph). Partitioning or pseudo-tearing may be accomplished by an appropriate ordering; in particular George (1973) suggested an ordering which is at least near-optimal in terms of the factorization count, and better than standard for storage: he reverse numbered the nodes in a series of separators, each of which is a minimal set of nodes such that it divides the largest possible block of connected nodes into two as nearly equally as possible. George entitled this process 'nested dissection' (ND), and it may be continued until no more such divisions are possible (see figure 3.7); it effectively corresponds to the hierarchical building up of systems envisioned by Kron (see above). It results in a rather more

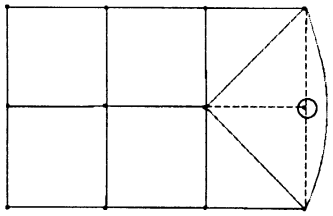

Figure 3.6 Graphical representation of Gaussian elimination of a row/column from a matrix: the corresponding node (circled) along with its incident edges (dashed) are removed; new edges (dotted) between nodes which had incident edges eliminated and were previously unconnected are added.

complicated matrix structure than that of the standard row-by-row ordering, somewhat similar to the 'orthogonal inverse' of Kron (1955) (cf. George, 1977, figure 3.3). Of more immediate interest, the leading order term in the estimated multiplication count for factorization is $O(n^3)$ and the storage requirement for the factor, or multiplication count for solution is $O(n^2 \ln n)$. The constants multiplying these leading order terms are quite large - George (1977) calculates about 10 for the factorization and 8 for the storage for the more complex finite element problem - but the impact of this is mitigated to some extent by significant lower order terms. In any case, as n increases we should observe increasing efficiency in both factorization and storage relative to the row-by-row ordering.

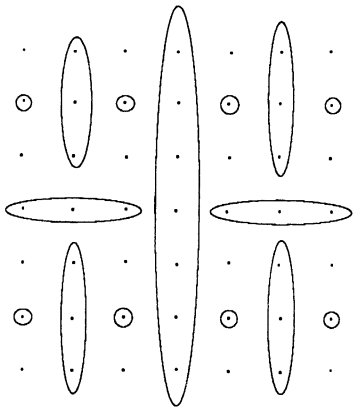

Figure 3.7 Demonstration of the set of separators used for the nested dissection of a 7×7 grid (after George, 1977). The uncircled nodes are to be eliminated first and then the encircled sets in order of increasing size.

Because of the apparently guaranteed computational advantage even for a one-off calculation, and lesser organizational complexity, a routine was written to perform factorization and/or solution of the matrices arising from the finite difference analogs of equations (3.5) and (3.6) on rectangular domains using the ND ordering. (The relative lack of flexibility of the kind inherent in the methods of diakoptics and MTRs was not perceived to be important.) In fact the routine was adapted from a similar one written for substitution into the magnetotelluric (MT) inversion program used by Jupp and Vozoff (1977). The MT context was used to explore the problems of adapting the algorithm from the relatively 'clean' world of numerical analysis, in which results seem to be proved for nice, real, positive definite matrices. Here underlying stability is apparently ensured by the physics of the problem, and the matrix is diagonally dominant, albeit non-Hermitian. However, the typical range of over 10 orders of magnitude in the diagonal elements was initially problematic: this was dealt with by factoring out the diagonal values, rescaling rows and columns as

$$P = CQC \quad ,$$

where

$$C = diag(\sqrt{P_{ii}}) \quad .$$

Thus, the problem of solving

$$P\mathbf{x} = \mathbf{s}$$

becomes that of solving

$$Q\mathbf{y} = C^{-1}\mathbf{s} \quad ,$$

where

$$\mathbf{y} = C\mathbf{x}$$

and Q has ones down its diagonal.

This routine reduced the runtime of the MT inversion by about 35% for a model with n about 40 and in excess of 50% for n about 60 (note that the numbers of rows and columns used in the program actually varies slightly with frequency, and are not equal in general). The results were essentially identical, so it appeared that stability problems were no longer significant.

The routine was further adapted for use with the RIM modelling described in this paper. The finite difference equations corresponding to (3.5) and (3.6) involve coupling between E and H values; by ordering them so that the two equations pertaining to a given point are consecutive, the matrix has the 2×2 block form of a single-variable finite difference problem. Therefore it is appropriate to use a block-graphical representation in which each node represents two rows and columns for the **E** and **H** values at each point and each edge a 2×2 off-diagonal non-zero matrix. This arrangement proved successful: there were again no stability problems and significant runtime savings were recorded despite the fact that the long, narrow shape of the models reduces the theoretical advantage of the ND ordering over the bandwidth-minimising row-by-row one. Our original inversion routine used the Greenfield algorithm (Greenfield, 1965), which is described in the appendix. The total time involved in such a solution is proportional to nm^3, where n is the number of horizontal nodes and m is the number of vertical nodes. For n and m equal to 31 the runtime saving using the nested dissection method was around 50% and about 80% for n and m equal to 67. (Table 1).

Matrix size	Time ratio
31×31	1:2
40×60	1:4
67×67	1:5

Table 1 The ratio of the time taken by the nested dissection method to that taken by the Greenfield algorithm

In general, for an $n \times n$ grid the effort involved in factorisation increases asymptotically as n^3 for nested dissection as against n^4 for the Greenfield method, and the effort for each solution after factorisation goes as $n^2 \ln n$ and n^3 respectively. In each case the proportionate saving offered by nested dissection increases with n, but the exact overall ratio will depend upon the number of nodes.

The method of nested dissection may also be applied to non-rectangular meshes (George and Liu, 1981), but require rather greater sophistication in programming than the routine used here.

4 Accuracy of the program

Results for a homogeneous space were tested against the analytic model and found to agree closely. For example, with $\sigma = 10^{-5}$ and source-receiver distances varying between 6 and 200 metres, agreement to better than 1 db (over a total range of 73 db) was obtained at all points.

For a 1D (uniformly layered) space the results were compared with those of K-H Lee (personal communication, 1986) whose program computes electromagnetic fields due to a dipole source anywhere in a uniformly layered earth. Typical agreement was better than 5%. Results were also compared against the analytic expression for the azimuthal component of the magnetic field given by Delogne (1982) and also by Hill(1984); this expression assumes normal mode propagation throughout the coal seam and so is not valid near the source. Beyond distances of the order of a few tens of metres the computed and analytic results agreed to graphical accuracy.

Finally a comparison was made with a model discussed by Greenfield and Wu (1988). As discussed below, agreement was quite satisfactory although the models were difficult to compare directly because Greenfield and Wu used a line source.

5 Results

Numerous geological models were examined and will be the subject of a later paper. Two of these models are considered in detail below. In both of these we have restricted ourselves to the case where the source and receiver are coplanar loops.

The first model is of a 4m thick coal seam interrupted by a vertical dyke of width 2m. The dyke was extended a distance of 1m above and below the coal seam. Conductivities were 0.0003 S/m for the coal, 0.003 S/m for the host rock and 0.05 S/m for the dyke, dielectric constants were set equal to unity and the frequency used was 300 kHz. This model was compared with results obtained for the same model using two other independent methods (figure 5.1). Method 1 due to G. Liu (personal communication, 1990) uses a line source rather than a dipole source. Method 2 uses a 3D model (Liu, personal communication, 1990). In this case the dyke was 60m long, symmetrically placed about the plane of the dipole. The excess attenuation near the dyke in all three cases was about 3.5db.

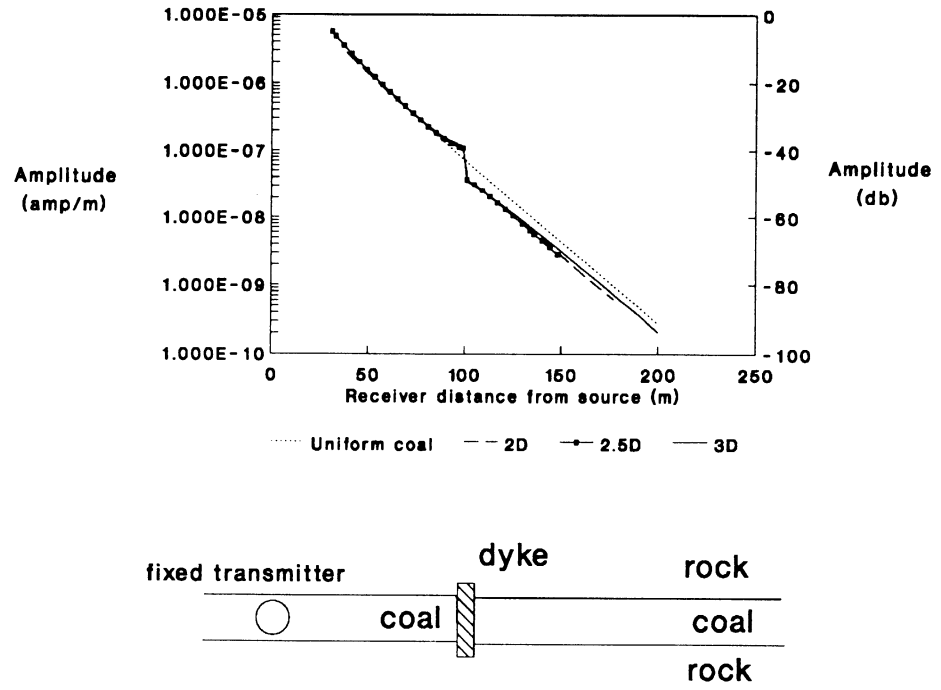

Figure 5.1 Comparison of three different numerical models for a coal seam broken by a dyke

We also considered the model of Greenfield and Wu (1988), in which a 40 metre segment of a coal seam was replaced by roof rock. The conductivities of rock and coal were respectively 0.001 and 0.00001 S/m, dielectric constants were 10 and 5 respectively and the seam thickness was 2 metres (figure 5.2).

Our (dipole source) model shows an excess attenuation of 5.7 db crossing the conductive zone, as compared with 7.0 db obtained by Greenfield and Wu using a line source. The decay rates also differ, but our rate, which agrees with those of Hill (1984), is the correct one. Given the large size of the anomaly, its effect is rather small, being less than half the size of that caused by the conductive dyke considered in section 2. Further, the phase changes only very slightly from that of uniform coal. This is a result of energy propagating partially through the rock and the effects are very sensitive to the conductivity of the rock.

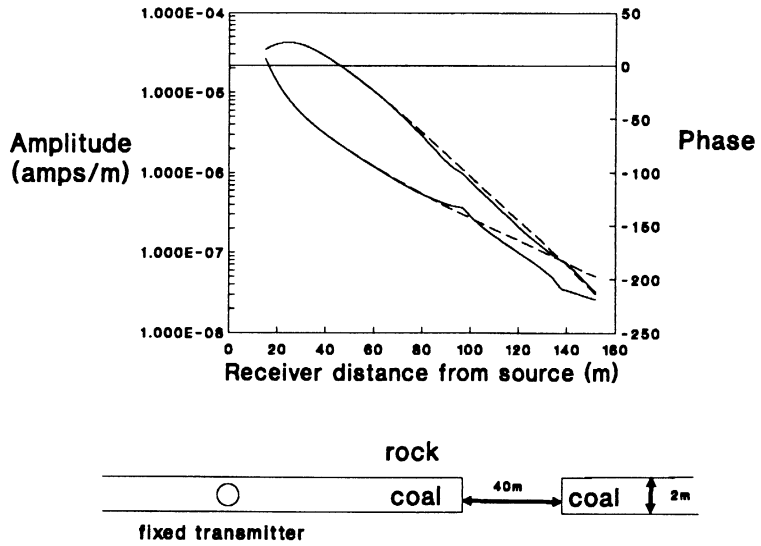

Figure 5.2 Model for which the coal seam has partially been replaced by roof rock. The upper curves represent the phase and the lower set represents the amplitude. Dashed curves are for uniform coal.

6 Conclusions

We have found that, as expected, the method of Nested Dissection offers significant runtime savings over more common methods. We have not found it to exhibit any stability problems.

We have used the method in an application to the currently important problem of wave propagation in coal seams which are disturbed geologically. As has been indicated, coals seams in many environments are often relatively unusual in their properties compared to the rocks above and below and, if they are undistorted by subsequent geological processes, they often form natural waveguides. We have demonstrated that typical geological disturbances which disrupt these waveguide characteristics are detectable using the radio imaging method (RIM) and that we can construct satisfactory models which agree with survey data. Finally, comparisons with analytic results and other numerical models indicate that our method is accurate.

7 Acknowledgements

Drs. Art Raiche and Steve Edwards originally suggested we investigate the use of graph theoretical methods in EM modelling problems. The present work was carried out in association with projects to evaluate the RIM method and associated imaging. Support was provided by a National Energy Research, Development and Demonstration Program contract to the Australian Coal Industry Research Laboratories and by Macquarie University, the University of Technology, Sydney and the Australian Research Council. We are indebted to the Commonwealth Scientific and Industrial

Research Organisation, Division of Radiophysics for the use of their Convex computer for the 3D modelling. We are grateful to Dr. Ki Ha Lee of the University of California, Berkeley for the use of his 1D program and to Dr. Peter Hatherly of ACIRL for organising the project. The 3D model program was written under contract by Dr. G. Newman; electrical property measurements were done under contract by Associate Professor D. Emerson. Finally, we are indebted to Dr. Giumin Liu and Jeanne Young for many useful discussions.

Appendix

The following discussion of the Greenfield algorithm is based on the description by Greenfield (1965)

The $2mn$ difference equations (3.7)and (3.8), which involve coupling between the electric and magnetic fields, are ordered so that two equations pertaining to a single node point are consecutive. The equations at grid point (i, j) are arranged in the order

$$\begin{array}{ccccc} (1,1) & (1',1') & \ldots & (1,n) & (1',n') \\ (2,1) & (2',1') & \ldots & (2,n) & (2',n') \\ \cdot & & & & \\ \cdot & & & & \\ \cdot & & & & \\ (m,1) & (m',1') & \ldots & (m,n) & (m',n') \end{array}$$

Here each unprimed (respectively primed) symbol refers to an equation of the type (3.7) (respectively (3.8)). Since each point is connected only to its neighbours, the set of equations is of the form

$$\mathbf{TV} = \mathbf{S} \quad ,$$

where the coefficient matrix $\mathbf{T}$ may be written in the partitioned form

$$\mathbf{T} = \begin{pmatrix} \mathbf{A}_1 & \mathbf{C}_1 & 0 & . & . & . & 0 \\ \mathbf{D}_1 & \mathbf{A}_2 & \mathbf{C}_2 & . & & & \\ 0 & \mathbf{D}_2 & \mathbf{A}_3 & . & . & . & . \\ . & . & . & . & . & . & . \\ . & . & . & . & . & . & . \\ . & . & . & . & . & . & . \\ . & . & . & . & 0 & \mathbf{D}_{n-1} & \mathbf{A}_n \end{pmatrix}$$

for certain $2m \times 2m$ square matrices $\mathbf{A}_k$,$\mathbf{C}_k$ and $\mathbf{D}_k$. Further, $\mathbf{C}_k$ and $\mathbf{D}_k$ are block diagonal with 2×2 blocks on the main diagonal. The matrices $\mathbf{V}$ and $\mathbf{S}$ correspond to field and source values respectively and may be partitioned as

$$\mathbf{V}=\begin{pmatrix}\mathbf{V}_1\\ \mathbf{V}_2\\ .\\ .\\ .\\ \mathbf{V}_n\end{pmatrix}, \qquad \mathbf{S}=\begin{pmatrix}\mathbf{S}_1\\ \mathbf{S}_2\\ .\\ .\\ .\\ \mathbf{S}_n\end{pmatrix}.$$

Here $\mathbf{V}_j$ and $\mathbf{S}_j$ are column vectors of length $2m$ with

$$\mathbf{V}_j=\begin{pmatrix}H_{1j}\\ E_{1j}\\ H_{2j}\\ E_{2j}\\ .\\ H_{mj}\\ E_{mj}\end{pmatrix}, \qquad \mathbf{S}_j=\begin{pmatrix}S_{1j}\\ S'_{1j}\\ .\\ .\\ .\\ S_{mj}\\ S'_{mj}\end{pmatrix}.$$

Each S_{ij} (respectively S'_{ij}) is zero unless there is a magnetic (respectively electric) source at grid point (i,j).

The matrix $\mathbf{T}$ is partitioned into two triangular matrices $\mathbf{E}$ and $\mathbf{F}$ according to

$$\mathbf{T}=\mathbf{EF}$$

with

$$\mathbf{E}=\begin{pmatrix}\mathbf{I} & 0 & . & . & . & 0\\ \mathbf{E}_1 & \mathbf{I} & . & . & . & .\\ 0 & \mathbf{E}_2 & \mathbf{I} & & & \\ . & . & . & & & \\ . & . & . & & & \\ 0 & . & . & 0 & \mathbf{E}_{n-1} & \mathbf{I}\end{pmatrix}, \quad \mathbf{F}=\begin{pmatrix}\mathbf{F}_1 & \mathbf{G}_1 & 0 & . & . & 0\\ 0 & \mathbf{F}_2 & \mathbf{G}_2 & . & . & \\ . & . & . & . & & \\ . & . & . & . & & \\ . & . & . & & & \\ 0 & . & . & . & 0 & \mathbf{F}_n\end{pmatrix}.$$

By comparing $\mathbf{T}$ and $\mathbf{EF}$ we readily find that

$$\mathbf{F}_1=\mathbf{A}_1 \qquad \mathbf{E}_1=\mathbf{D}_1\mathbf{F}_1^{-1}$$

$$\mathbf{F}_2=\mathbf{A}_2-\mathbf{E}_1\mathbf{G}_1 \qquad \mathbf{E}_2=\mathbf{D}_2\mathbf{F}_2^{-1}$$

$$. \qquad .$$

$$. \qquad .$$

$$\mathbf{F}_n=\mathbf{A}_n-\mathbf{E}_{n-1}\mathbf{G}_{n-1} \qquad \mathbf{E}_{n-1}=\mathbf{D}_{n-1}\mathbf{F}_{n-1}^{-1}$$

If we now define a vector **Z** by

$$\mathbf{FV} = \mathbf{Z} = \begin{pmatrix} \mathbf{Z}_1 \\ \mathbf{Z}_2 \\ \cdot \\ \cdot \\ \cdot \\ \mathbf{Z}_n \end{pmatrix} ,$$

where the $\mathbf{Z}_k$ are column vectors of length n, then we have

$$\mathbf{Z}_1 = \mathbf{S}_1$$

$$\mathbf{Z}_k = \mathbf{S}_k - \mathbf{E}_{k-1}\mathbf{Z}_{k-1} \qquad k = 2, 3, \ldots, m$$

and we can find the required solution **V** by

$$\mathbf{V}_n = \mathbf{F}_n^{-1}\mathbf{Z}_n$$

$$\mathbf{V}_k = \mathbf{F}_k^{-1}(\mathbf{Z}_k - \mathbf{G}_k\mathbf{V}_{k+1}) \qquad k = m-1, m-2, \ldots, 1 \quad .$$

The operations which require the main bulk of the computation are the matrix multiplications $\mathbf{D}_k\mathbf{F}_k^{-1}$ and the inversion of the matrix $\mathbf{F}_k$. Both of these operations increase as m^3 and have to be done n times, so that the total number of operations increases as nm^3.

References

Asten, M.W., Drake, L.A. & Edwards, S.A. (1984): "In seam seismic Love wave propagation modelled by the finite element method", Geophysical *Prospecting,* **32**, 649-661

Brewitt-Taylor, C.R. & Johns, P.B. (1978): "Diakoptic Solution of Induction Problems", *J.Geomag. Geoelect. Suppl. 1*, **32**, 73-78.

Bunch, J.R. & Rose, D.J. (1974): "Partitioning, tearing and modification of sparse linear systems", *J.Math.Anal.Appl.*, **48**, 574-593.

Delogne, P.(1982): "Leaky feeders and subsurface radio communications", *Peter Periginus Ltd, IEE electromagnetic waves series, #14.*

Edwards, S.A., Asten, M.W. & Drake, L.A. (1985): "P-SV wave scattering by coal seam inhomogenieties", *Geophysics* **50**, 214-223.

Emslie, A.G.and Lagace, R.L., "Propagation of low and medium frequency radio waves in a coal seam",(1976) *Radio Science,* **11**, 253-261

George, A. (1973): "Nested Dissection of a regular finite element mesh", *SIAM J.Numer.Anal.*, **10**, 345-363.

George, A. (1977): "Numerical experiments using dissection methods to solve *n* by *n* grid problems", *SIAM J.Numer.Anal.*, **14**, 161-179.

George, A and Liu, J. W. (1981): "Computer Solution of Large Sparse Positive Definite Systems", *Englewood Cliffs: Prentice-Hall.*

Greenfield, R.J. (1965), "Two dimensional calculations of magnetic micropulsation resonances", *Ph.D thesis, M.I.T.*

Greenfield, R. J. and Wu, S. T (1988):"Electromagnetic wave propagation in disrupted coal seams", *SEG Annual meeting, Expanded Technical Abstract EM 1.7.*

Hatherly, P. J. (1987): "Development of electromagnetic techniques for the location of geological discontinuities in coal mines", *Report to the Australian Coal Association.*

Hill, D. A. (1984): "Radio propagation in a coal seam and the inverse problem", *Journal of Research of the NBS,* **89,** 385-394.

Hill, D. A. (1986): "Electromagnetic wave propagation in am asymmetrical coal seam", *IEEE Transactions on Antennas and Propagation,* **AP-34**, 244-247

Hohmann, G.W.(1988), "Numerical modelling for electromagnetic methods of geophysics" In: *Electromagnetic methods in applied geophysics I; Society of Exploration Geophysicists.*

Jupp, D.L.B. & Vozoff, K. (1977): "Two-dimensional magnetotelluric inversion", *Geophys. J. R. Astr. Soc.*, **50**, 333-352.

Kesavan, H.K. & Dueckman, J. (1982): "Multi-terminal representations and diakoptics", *J.Franklin Inst.*, **313**, 337-352.

Kron, G. (1955): "Inverting a 256×256 matrix", *Engineering*, **178**, 309-312.

Kron, G. (1963): *Diakoptics: the piecewise solution of large-scale systems*, Macdonald, London.

Liu, G. M., Smith, G. H.,Thomson, S., Vozoff, K. & Hatherly, P. (1991): "A numerical study of electromagnetic wave propagation (RIM) in disrupted coal seams", *Exploration Geophysics* (submitted).

Madden, T.R. (1972): "Transmission systems and network analogies to geophysical forward and inverse problems", *Technical Report no. 72-3*, Dept. Earth and Planetary Sciences, Massachusetts Inst. Technology, Cambridge, Mass. 02139.

Madden, T.R. & Mackie, R.L. (1989): "Three-dimensional magnetotelluric modeling and inversion", *Proc.IEEE*, **77**, 318-333.

Savage, G.J. & Kesavan, H.K. (1979): "The graph theoretic field model - I: Modelling and formulations", *J.Franklin Inst.*, **302**, 107-147.

Savage, G.J. & Kesavan, H.K. (1980): "The graph theoretic field model - II: Application of multiterminal representations to field problems", *J.Franklin Inst.*, **309**, 241-266.

Shope, S. M.(1987): "Electromagnetic coal seam tomography", *Ph.D thesis, Pennsylvania State University.*

Shope, S. A., Greenfield, R. J.& Stolarczyk, L.(1986): "Use of electromagnetic waves for longwall coal seam tomography", *56th Annual SEG meeting, Extended Abstracts.*

Stolarczyk, L.(1986): "Continuous wave medium frequency signal transmission survey procedure for imaging structure in coal seams", U.S. Patent No.4,577,153

Stoyer,C. H. and Greenfield, R. J. (1976): "Numerical solutions of the response of a two dimensional earth to an oscillating magnetic dipole source", *Geophysics* **41** 519-530.